January 13, 2017

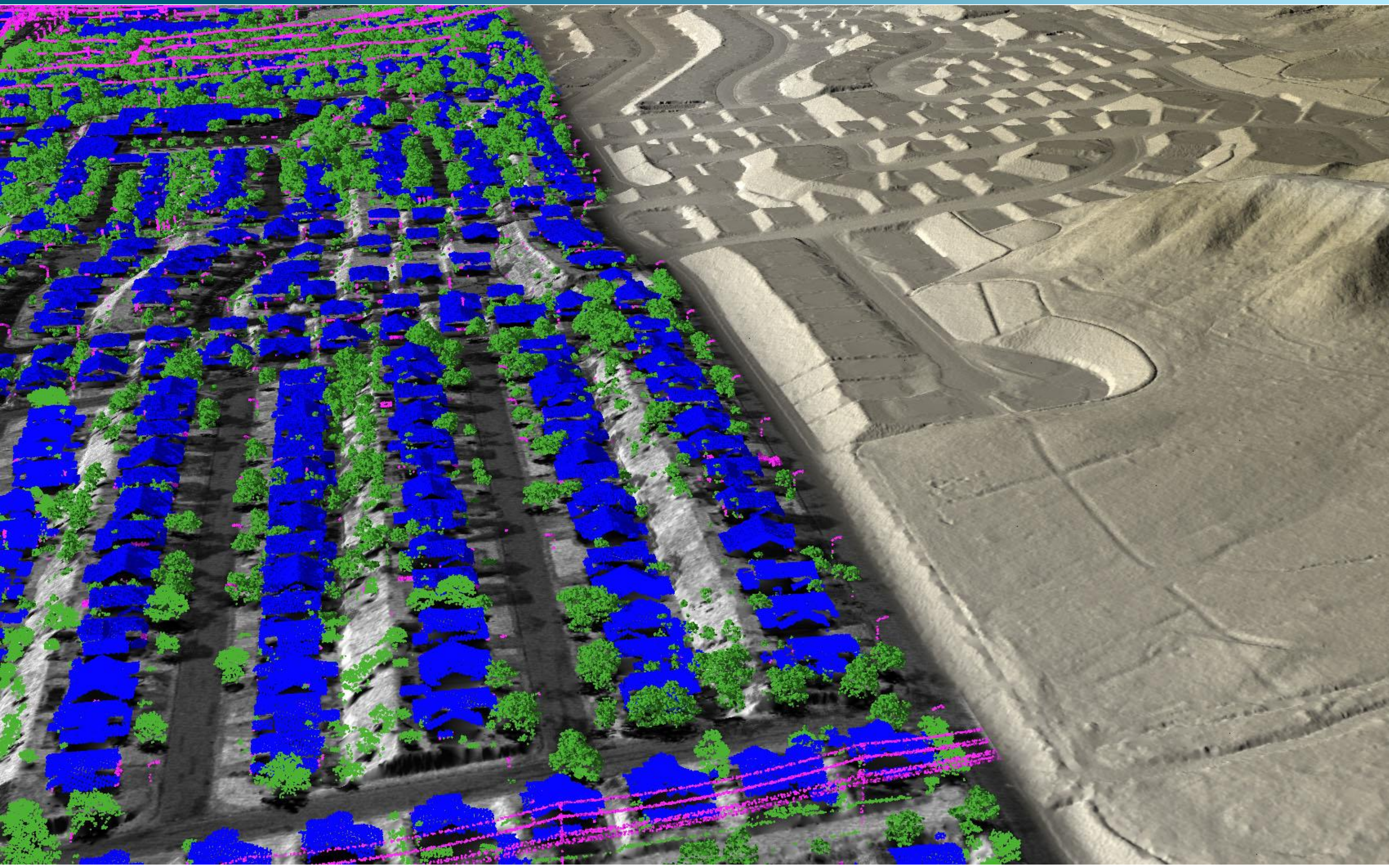

California High Speed Rail – South AOI
LiDAR Technical Data Report

Neal Driscoll
Scripps Institution of Oceanography-U.C. San Diego
9500 Gilman Drive #0244
La Jolla, CA 92093-0244
PH: 541-752-1204

QSI Corvallis
517 SW 2nd St., Suite 400
Corvallis, OR 97333
PH: 541-752-1204

Table of Contents

Cover Photo: A two part view of the Desert View Highlands community; the right half of the image displays the gridded bare earth surface of the project area, while the left half of the image includes the overlaid LiDAR point cloud colored by intermediate point classification.

INTRODUCTION

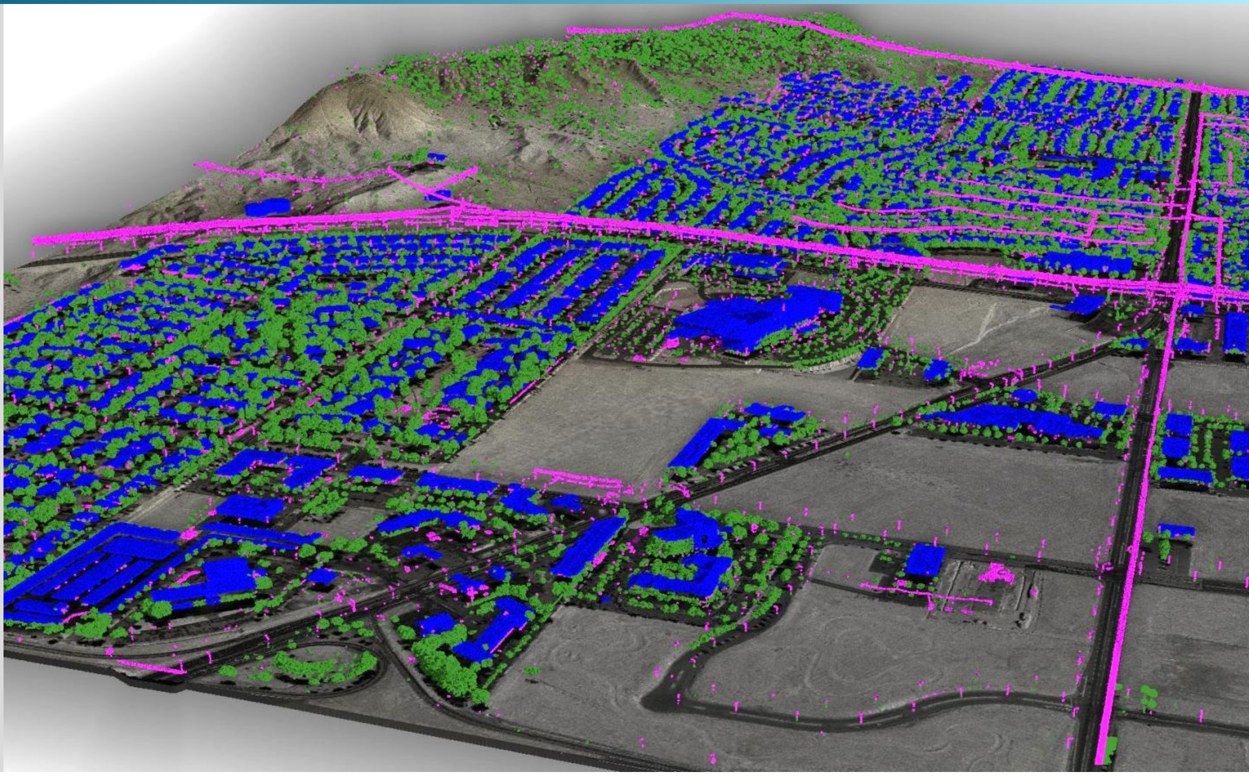

This image shows a view of the California High Speed Rail South project area, created from the gridded bare earth surface and above-ground LiDAR point cloud colored by intermediate point classification.

In August 2016, Quantum Spatial (QSI) was contracted by the University of California – San Diego (UCSD) to collect Light Detection and Ranging (LiDAR) data in the fall of 2016 for two California High Speed Rail sites in Southern California. The data were split into two deliveries: north and south, respectively. Data were collected to aid UCSD in assessing the topographic and geophysical properties of the study area to support geological and seismological evaluation of the proposed high speed rail line sites.

The California High Speed Rail North area of interest (AOI) was delivered to UCSD on December 12th, 2016. This report accompanies the delivered LiDAR data for the California High Speed Rail South AOI, and concludes the LiDAR acquisition and processing phases of this project. Documented herein are contract specifications, data acquisition procedures, processing methods, and analysis of the final dataset including LiDAR accuracy and density. Acquisition dates and acreage are shown in Table 1, a complete list of contracted deliverables provided to UCSD is shown in Table 2, and the project extent is shown in Figure 1 and Figure 2.

Table 1: Acquisition dates, acreage, and data types collected on the California High Speed Rail – South AOI

Project Site	Contracted Acres	Buffered Acres	Acquisition Dates	Data Type	Delivery Date
California High Speed Rail – South AOI	323,647	319,938	08/27/2016 – 09/12/2016, 09/17/2016	LiDAR	January 16th, 2017

Deliverable Products

Table 2: Products delivered to UCSD for the California High Speed Rail – South AOI

California High Speed Rail – South AOI Products Projection: California State Plane Zone 5 Horizontal Datum: NAD83 (NSRS2007) Vertical Datum: NAVD88 (GEOID09) Units: US Survey Feet	
Points	LAS v 1.2 • All Classified Returns
Rasters	3 Foot ESRI Grids • Bare Earth Model • Highest Hit Model 1.5 Foot GeoTiffs • Intensity Images
Vectors	Shapefiles (*.shp) • Site Boundary • LiDAR Tile Index (2250 ft x 2250 ft) • Water's Edge Polygon

Figure 1: Location map of the California High Speed Rail South AOI, between Bakersfield and Los Angeles, California

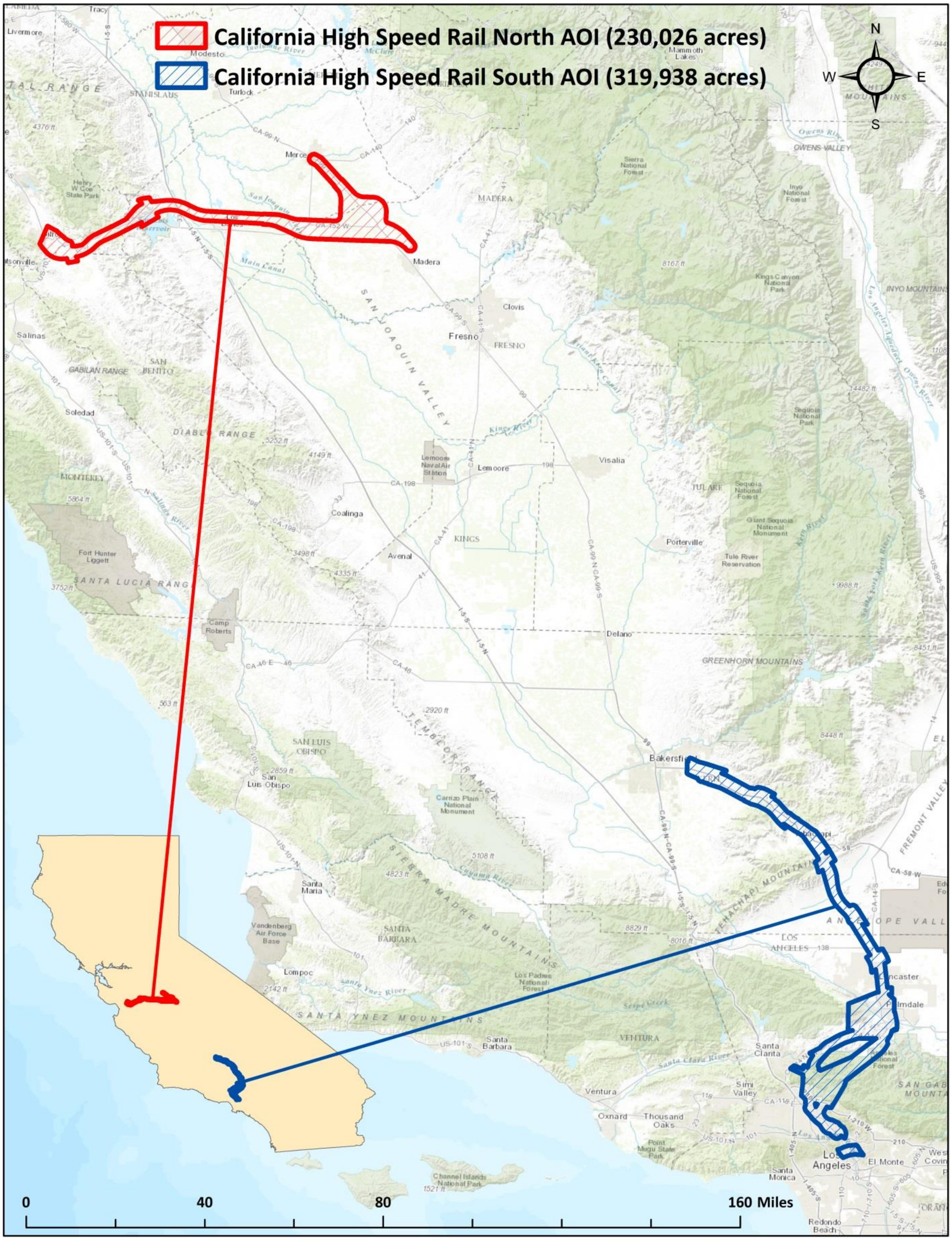

Figure 2: Location Map of the California High Speed Rail Project Sites

Acquisition

QSI's Cessna Caravan (left) and Partenavia P-68 (right) aircraft used to acquire LiDAR data over the California High Speed Rail South AOI

Planning

In preparation for data collection, QSI reviewed the project area and developed a specialized flight plan to ensure complete coverage of the South AOI of the California High Speed Rail LiDAR study area at the target point density of ≥8.0 points/m^2 (0.74 points/ft^2). Acquisition parameters including orientation relative to terrain, flight altitude, pulse rate, scan angle, and ground speed were adapted to optimize flight paths and flight times while meeting all contract specifications.

Factors such as satellite constellation availability and weather windows must be considered during the planning stage. Any weather hazards or conditions affecting the flights were continuously monitored due to their potential impact on the daily success of airborne and ground operations. In addition, logistical considerations including private property access and potential air space restrictions were reviewed.

Airborne LiDAR Survey

The LiDAR survey was accomplished using a Leica ALS80 system mounted in a Cessna Caravan and Partenavia P-68. Table 3 summarizes the settings used to yield an average pulse density of ≥8.0 points/m^2 (0.74 points/ft^2) over the California High Speed Rail – South AOI project area. The Leica ALS80 laser system can record unlimited range measurements (returns) per pulse. It is not uncommon for some types of surfaces (e.g., dense vegetation or water) to return fewer pulses to the LiDAR sensor than the laser originally emitted. The discrepancy between first return and overall delivered density will vary depending on terrain, land cover, and the prevalence of water bodies. All discernible laser returns were processed for the output dataset.

Table 3: LiDAR specifications and survey settings

LiDAR Survey Settings & Specifications		
Acquisition Dates	August 27 – September 12, 2016	September 17, 2016
Aircraft Used	Partenavia P-68	Cessna Caravan
Sensor	Leica	Leica
Laser	ALS80	ALS80
Maximum Returns	Unlimited	Unlimited
Resolution / Density	Average 8 pulses/m^2	Average 8 pulses/m^2
Nominal Pulse Spacing	0.35 m	0.35 m
Survey Altitude (AGL)	1600 m	1600 m
Survey Speed	110 knots	105 knots
Field of View	40^o	40^o
Mirror Scan Rate	52 Hz	46 Hz
Target Pulse Rate	335.6 kHz	320 kHz
Pulse Length	2.5 ns	2.5 ns
Laser Pulse Footprint Diameter	35 cm	35 cm
Central Wavelength	1064	1064
Pulse Mode	Multi Pulse in Air (MPIA)	Multi Pulse in Air (MPIA)
Beam Divergence	22 mrads	22 mrads
Swath Width	1,165 m	1,165 m
Swath Overlap	67%	71%
GPS Baselines	≤13 nm	≤13 nm
GPS PDOP	≤3.0	≤3.0
GPS Satellite Constellation	≥6	≥6
Maximum Returns	Unlimited	Unlimited
Intensity	8-bit scaled to 16-bit	8-bit scaled to 16-bit
Accuracy	$RMSE_Z \leq 9$ cm	$RMSE_Z \leq 9$ cm

All areas were surveyed with an opposing flight line side-lap of ≥50% (≥100% overlap) in order to reduce laser shadowing and increase surface laser painting. To accurately solve for laser point position (geographic coordinates x, y and z), the positional coordinates of the airborne sensor and the attitude of the aircraft were recorded continuously throughout the LiDAR data collection mission. Position of the aircraft was measured twice per second (2 Hz) by an onboard differential GPS unit, and aircraft attitude was measured 200 times per second (200 Hz) as pitch, roll and yaw (heading) from an onboard inertial measurement unit (IMU). To allow for post-processing correction and calibration, aircraft and sensor position and attitude data are indexed by GPS time.

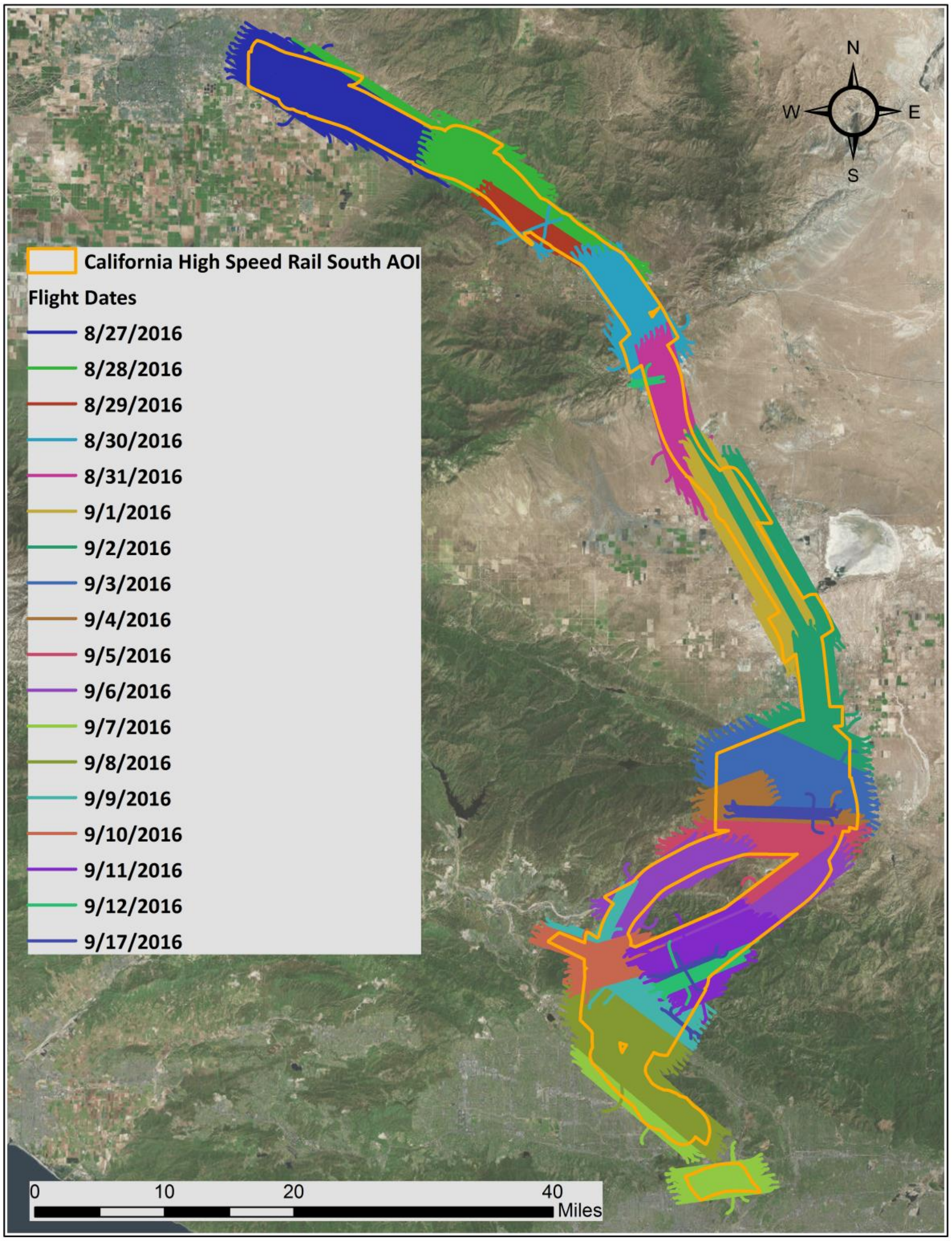

Figure 3: Flightline map for the California High Speed Rail LiDAR project, South AOI

Ground Control

Ground control surveys, including monumentation and ground survey points (GSPs) were conducted to support the airborne acquisition. Ground control data were used to geospatially correct the aircraft positional coordinate data and to perform quality assurance checks on final LiDAR data.

All ground surveys were tied to the CA HSR primary control network.

Monumentation

The spatial configuration of ground survey monuments provided redundant control within 13 nautical miles of the mission areas for LiDAR flights. Monuments were also used for collection of GSPs using real time kinematic (RTK), post processed kinematic (PPK) and fast static (FS) survey techniques.

Monument locations were selected with consideration for satellite visibility, field crew safety, and optimal location for GSP coverage. QSI utilized nine HSR primary control points, five existing supplemental control points, one UNAVCO Plate Boundary Observatory (PBO) CORS, and ten newly-established supplemental control points in the South AOI of the California High Speed Rail LiDAR project (Table 4, Figure 5). QSI's professional land surveyor, Tom Tucker (CAPLS#4460) oversaw and certified the utilization of all monuments.

Table 4: Monuments utilized for the California High Speed Rail – South AOI acquisition. Coordinates are on the NAD83 (NSRS2007) datum, epoch 2002.00.

Monument ID	Mark Type	Latitude	Longitude	Ellipsoid (meters)
CA_HSR_06	QSI Supplemental	34° 29' 30.03808"	-118° 16' 53.23425"	857.533
CAL_HSR_01	QSI Supplemental	35° 17' 36.63378"	-118° 45' 08.89943"	238.870
CAL_HSR_02	QSI Supplemental	35° 15' 51.60305"	-118° 40' 02.14111"	526.850
CAL_HSR_03	QSI Supplemental	35° 11' 58.10332"	-118° 31' 18.81869"	920.205
CAL_HSR_04	QSI Supplemental	34° 50' 56.79604"	-118° 15' 07.78366"	695.621
CAL_HSR_05	QSI Supplemental	34° 53' 10.18276"	-118° 17' 27.95191"	765.978
CAL_HSR_07	QSI Supplemental	34° 14' 49.95947"	-118° 24' 06.99260"	245.635
CAL_HSR_08	QSI Supplemental	34° 15' 59.52469"	-118° 20' 07.02825"	332.899
CAL_HSR_09	QSI Supplemental	34° 19' 53.18948"	-118° 20' 28.80323"	581.641
CAL_HSR_10	QSI Supplemental	34° 24' 49.35408"	-118° 26' 30.87750"	418.119
D316P	HSR Primary	35° 19' 31.18825"	-118° 46' 39.03954"	242.962
D346P	HSR Primary	35° 08' 44.32951"	-118° 26' 56.41331"	1176.148
D356P	HSR Primary	35° 05' 54.70658"	-118° 17' 37.34609"	1132.197
D366P	HSR Primary	34° 59' 39.46801"	-118° 09' 20.44174"	771.105
D376P	HSR Primary	34° 50' 04.29632"	-118° 10' 00.58022"	675.396
D395P	HSR Primary	34° 34' 46.90544"	-118° 07' 35.48556"	785.439

Monument ID	Mark Type	Latitude	Longitude	Ellipsoid (meters)
D397P	HSR Primary	34° 32' 45.38254"	-118° 07' 51.68396"	876.943
D421P	HSR Primary	34° 21' 51.66837"	-118° 30' 02.49066"	404.081
D428P	HSR Primary	34° 16' 44.53841"	-118° 26' 09.81259"	286.923
EW0537	QSI Supplemental	34° 44' 01.36380"	-118° 08' 31.12065"	673.272
EW0552	QSI Supplemental	34° 42' 15.03232"	-118° 11' 32.86873"	674.679
EW2625	QSI Supplemental	34° 27' 55.12559"	-118° 11' 47.84864"	791.326
FU0387	QSI Supplemental	35° 07' 21.51817"	-118° 22' 42.48543"	1184.344
P517	PBO CORS	34° 22' 34.90109"	-118° 10' 39.20737"	1959.870
PGE_PIPE_67	QSI Supplemental	35° 02' 37.17491"	-118° 18' 42.81847"	1099.356

To correct the continuously recorded onboard measurements of the aircraft position, QSI concurrently conducted multiple static Global Navigation Satellite System (GNSS) ground surveys (1 Hz recording frequency) over each monument. During post-processing, the static GPS data were triangulated with nearby Continuously Operating Reference Stations (CORS) using the Online Positioning User Service (OPUS[1]) for precise positioning. Multiple independent sessions over the same monument were processed to confirm antenna height measurements and to refine position accuracy.

Monuments were established according to the national standard for geodetic control networks, as specified in the Federal Geographic Data Committee (FGDC) Geospatial Positioning Accuracy Standards for geodetic networks.[2] This standard provides guidelines for classification of monument quality at the 95% confidence interval as a basis for comparing the quality of one control network to another. The monument rating for this project is shown in Table 5.

Table 5: Federal Geographic Data Committee monument rating for network accuracy

Direction	Rating
1.96 * St Dev $_{NE}$:	0.020 m
1.96 * St Dev $_{z}$:	0.050 m

For the South AOI of the California High Speed Rail LiDAR project, the monument coordinates contributed no more than the rated error to the geolocation of the final ground survey points and LiDAR, with 95% confidence.

[1] OPUS is a free service provided by the National Geodetic Survey to process corrected monument positions. http://www.ngs.noaa.gov/OPUS.

[2] Federal Geographic Data Committee, Geospatial Positioning Accuracy Standards (FGDC-STD-007.2-1998). Part 2: Standards for Geodetic Networks, Table 2.1, page 2-3. http://www.fgdc.gov/standards/projects/FGDC-standards-projects/accuracy/part2/chapter2

Network Evaluation

All ground survey data was tied to the HSR control network using static GNSS occupations of HSR Primary Control points. Each Primary Control point was occupied with two or more static sessions of at least two hours in length unless otherwise noted below. These sessions were processed against the NGS CORS using the OPUS Projects utility and transformed from NAD83(2011)(Epoch2010.00) to the NAD83(2007)(Epoch2007.00) realization using the NGS HTDP utility.

These updated coordinates were compared to the HSR Primary Control network record coordinates and evaluated for validity (Table 6). Differences were determined by subtracting record coordinates from the newly computed coordinates. Differences between HSR and QSI coordinates were within the normal tolerances of a geodetic survey, and the record HSR coordinates were held as intended.

Table 6: Evaluation of HSR Primary Control for California High Speed Rail – South AOI

Mark	∆N (m)	∆E (m)	∆Z (m)
D316P	0.019	-0.010	-0.012
D346P	0.001	-0.003	0.024
D356P*	0.015	-0.015	0.025
D366P	-0.008	-0.015	0.048
D376P*	-0.005	-0.004	0.045
D395P	0.016	-0.032	0.025
D397P	0.018	0.002	0.029
D421P*	-0.018	-0.033	-0.021
D428P	-0.001	-0.012	0.024

*Note: Starred marks were tied using fast-static survey techniques and used to check final products.

Ground Survey Points (GSPs)

Ground survey points were collected using real time kinematic (RTK), post-processed kinematic (PPK), and fast-static (FS) survey techniques. A Trimble R7 base unit was positioned at a nearby monument to broadcast a kinematic correction to a roving Trimble R10 GNSS receiver. All GSP measurements were made during periods with a Position Dilution of Precision (PDOP) of ≤ 3.0 with at least six satellites in view of the stationary and roving receivers. When collecting RTK and PPK data, the rover records data while stationary for five seconds, then calculates the pseudorange position using at least three one-second epochs. FS surveys record observations for up to fifteen minutes on each GSP in order to support longer baselines for post-processing. Relative errors for any GSP position must be less than 1.5 cm horizontal and 2.0 cm vertical in order to be accepted. See Table 7 for Trimble unit specifications.

GSPs were collected in areas where good satellite visibility was achieved on paved roads and other hard surfaces such as gravel or packed dirt roads. GSP measurements were not taken on highly reflective surfaces such as center line stripes or lane markings on roads due to the increased noise seen in the laser returns over these surfaces. GSPs were collected within as many flightlines as possible; however the distribution of GSPs depended on ground access constraints and monument locations and may not be equitably distributed throughout the study area (Figure 5).

Table 7: Trimble equipment identification

Receiver Model	Antenna	OPUS Antenna ID	Use
Trimble R7	Zephyr GNSS Geodetic Model 2 RoHS	TRM57971.00	Static
Trimble R10 GNSS	Integrated Antenna R10	TRMR10	Static, Rover

Figure 4: A photo taken by the QSI acquisition team of a Trimble R7 base station set up within the California High Speed Rail South AOI

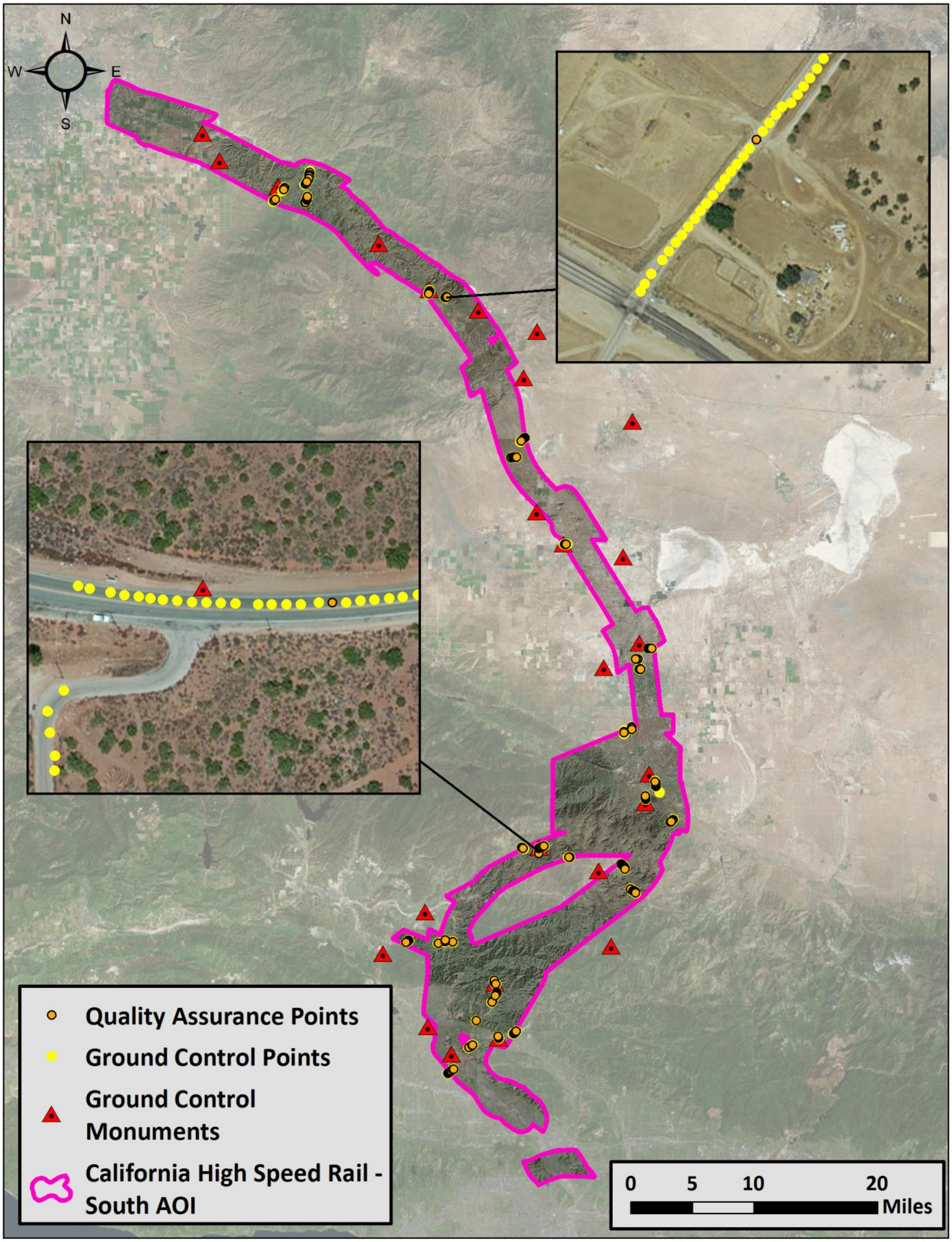

Figure 5: Ground Survey Location Map for California High Speed Rail South AOI

This LiDAR cross section shows a view of the California High Speed Rail South project area, colored by point classification.

LiDAR Data

Upon completion of data acquisition, QSI processing staff initiated a suite of automated and manual techniques to process the data into the requested deliverables. Processing tasks included GPS control computations, smoothed best estimate trajectory (SBET) calculations, kinematic corrections, calculation of laser point position, sensor and data calibration for optimal relative and absolute accuracy, and LiDAR point classification (Table 8). Processing methodologies were tailored for the landscape. Brief descriptions of these tasks are shown in Table 9.

Table 8: ASPRS LAS classification standards applied to the California High Speed Rail – South AOI dataset

Classification Number	Classification Name	Classification Description
1	Default/Unclassified	Laser returns that are not included in the ground class, composed of vegetation and anthropogenic features that are not buildings
2	Ground	Laser returns that are determined to be ground using automated and manual cleaning algorithms
3	Low Vegetation	Any vegetation between 2 – 5m of the ground surface
5	High Vegetation	Any vegetation greater than 5m above the ground surface
6	Buildings	Permanent structures with area ≥20m²
7	Noise	Laser returns that are often associated with birds, scattering from reflective surfaces, or artificial points below the ground surface.
9	Water	Laser returns that are determined to be water using automated and manual cleaning algorithms
10	Ignored Ground	Ground points proximate to water's edge breaklines

Table 9: LiDAR processing workflow

LiDAR Processing Step	Software Used
Resolve kinematic corrections for aircraft position data using kinematic aircraft GPS and static ground GPS data. Develop a smoothed best estimate of trajectory (SBET) file that blends post-processed aircraft position with sensor head position and attitude recorded throughout the survey.	Waypoint Inertial Explorer v.8.6
Calculate laser point position by associating SBET position to each laser point return time, scan angle, intensity, etc. Create raw laser point cloud data for the entire survey in *.las (ASPRS v. 1.2) format. Convert data to orthometric elevations by applying a geoid correction.	Waypoint Inertial Explorer v.8.6 Leica Cloudpro v. 1.2.2
Import raw laser points into manageable blocks (less than 500 MB) to perform manual relative accuracy calibration and filter erroneous points. Classify ground points for individual flight lines.	TerraScan v.16
Using ground classified points per each flight line, test the relative accuracy. Perform automated line-to-line calibrations for system attitude parameters (pitch, roll, heading), mirror flex (scale) and GPS/IMU drift. Calculate calibrations on ground classified points from paired flight lines and apply results to all points in a flight line. Use every flight line for relative accuracy calibration.	TerraMatch v.16
Classify resulting data to ground and other client designated ASPRS classifications (Table 8). Assess statistical absolute accuracy via direct comparisons of ground classified points to ground control survey data.	TerraScan v.16 TerraModeler v.16
Generate bare earth models as triangulated surfaces. Generate highest hit models as a surface expression of all classified points. Export all surface models as ESRI GRIDs format at a 3.0 foot pixel resolution.	TerraScan v.16 TerraModeler v.156 ArcMap v. 10.2
Correct intensity values for variability and export intensity images as GeoTIFFs at a 1.5 foot pixel resolution.	Las Monkey 2.2.1SP2 (QSI proprietary) LAS Product Creator 1.5 (QSI proprietary) ArcMap v. 10.2

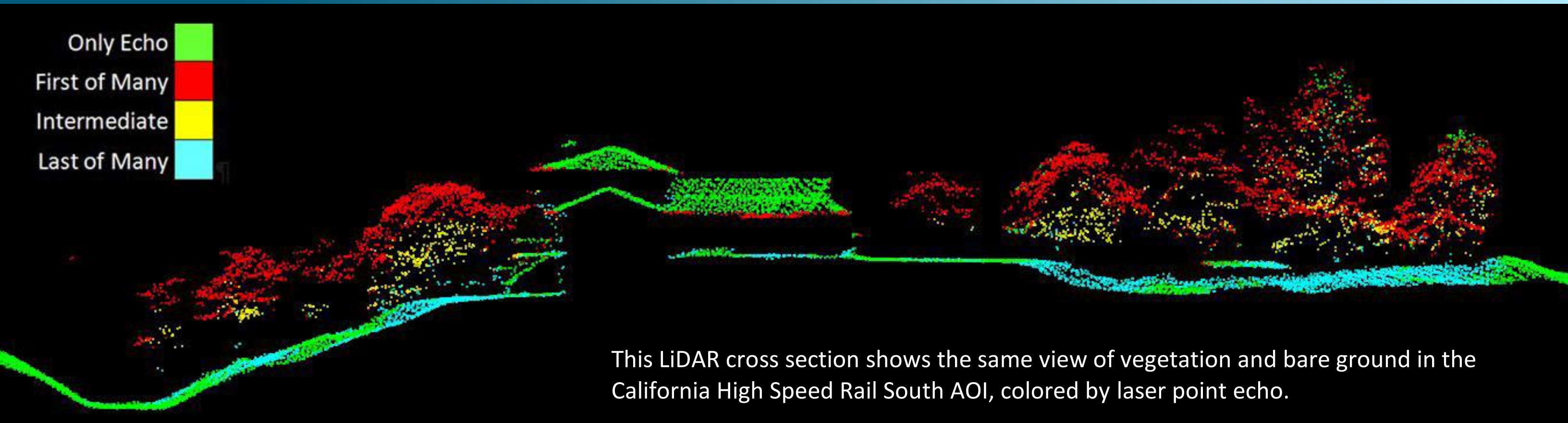

This LiDAR cross section shows the same view of vegetation and bare ground in the California High Speed Rail South AOI, colored by laser point echo.

LiDAR Density

The acquisition parameters were designed to acquire an average first-return density of 8 points/m^2 (0.74 points/ft^2). First return density describes the density of pulses emitted from the laser that return at least one echo to the system. Multiple returns from a single pulse were not considered in first return density analysis. Some types of surfaces (e.g., breaks in terrain, water and steep slopes) may have returned fewer pulses than originally emitted by the laser. First returns typically reflect off the highest feature on the landscape within the footprint of the pulse. In forested or urban areas the highest feature could be a tree, building or power line, while in areas of unobstructed ground, the first return will be the only echo and represents the bare earth surface.

The density of ground-classified LiDAR returns was also analyzed for this project. Terrain character, land cover, and ground surface reflectivity all influenced the density of ground surface returns. In vegetated areas, fewer pulses may penetrate the canopy, resulting in lower ground density.

The average first-return density of LiDAR data for the California High Speed Rail – South AOI was 1.43 points/ft^2 (12.84 points/m^2) while the average ground classified density was 0.32 points/ft^2 (2.91 points/m^2) (Table 10). The statistical and spatial distributions of first return densities and classified ground return densities per 300 x 300 foot cell are portrayed in Figure 6 through Figure 8.

Table 10: Average LiDAR point densities

Classification	Point Density
First-Return	1.43 points/ft^2 12.84 points/m^2
Ground Classified	0.32 points/ft^2 2.91 points/m^2

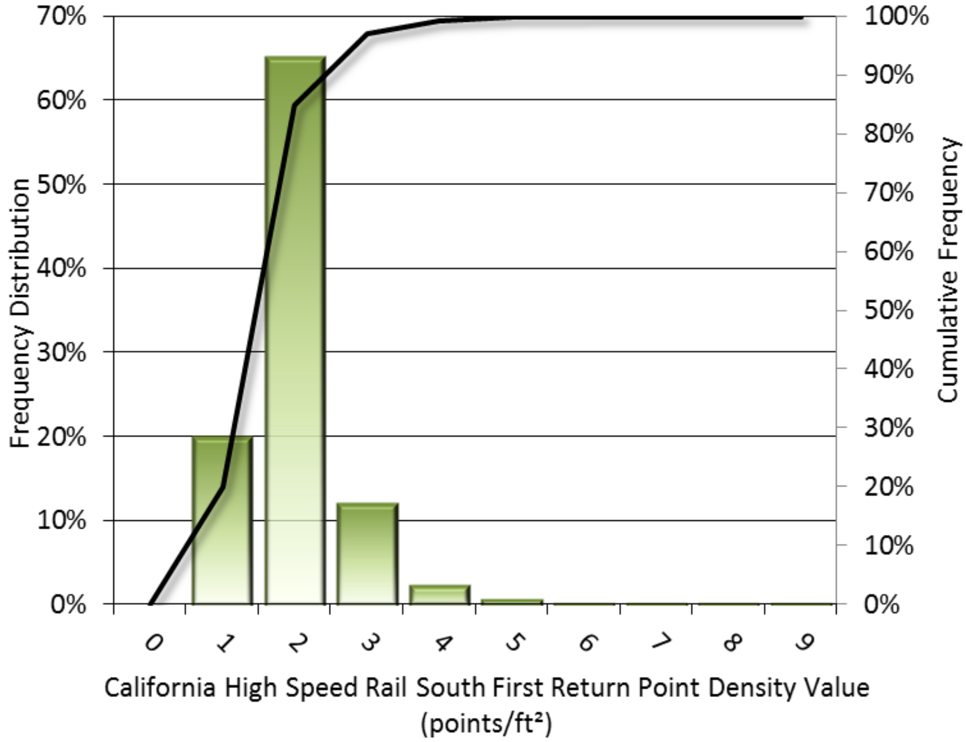

Figure 6: Frequency distribution of first return point density values per 300 x 300 ft cell

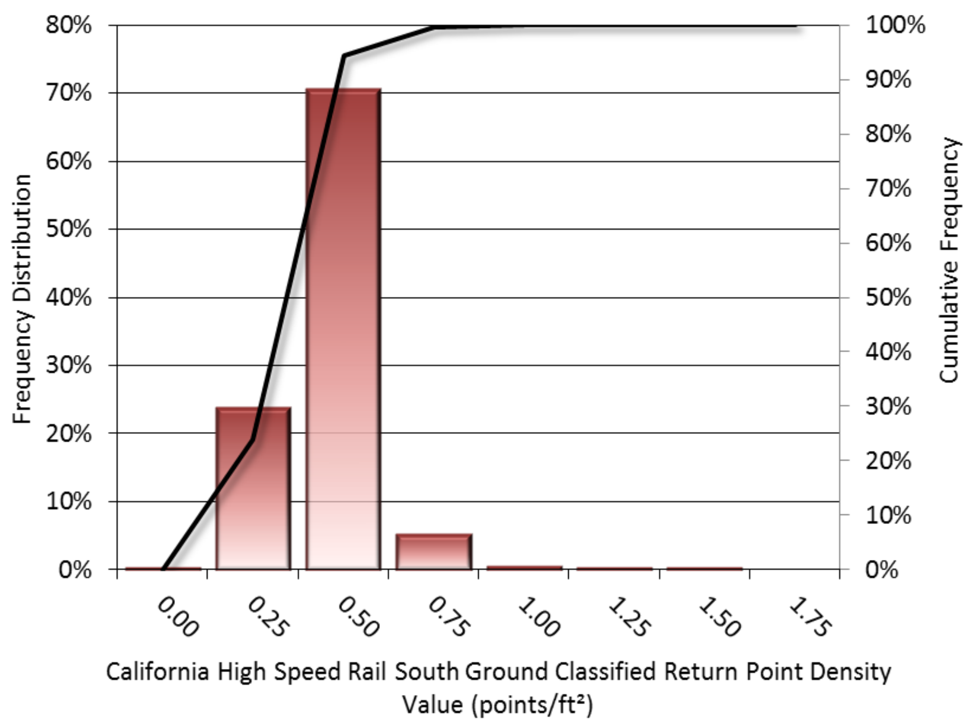

Figure 7: Frequency distribution of ground-classified return point density values per 300 x 300 ft cell

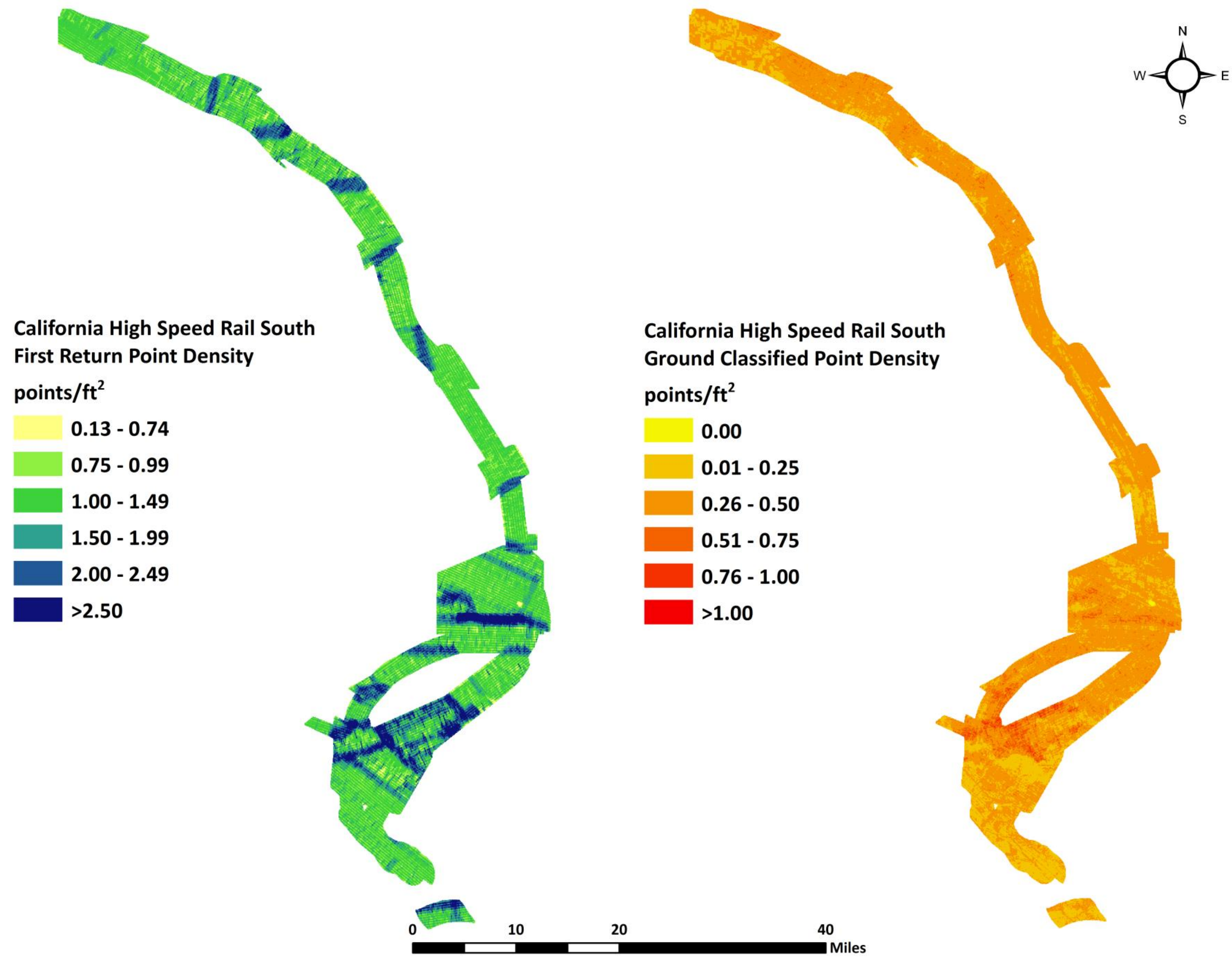

Figure 8: Ground classified and First return density map for the California High Speed Rail – South AOI (300 ft x 300 ft cells)

LiDAR Accuracy Assessments

The accuracy of the LiDAR data collection can be described in terms of absolute accuracy (the consistency of the data with external data sources) and relative accuracy (the consistency of the dataset with itself). See Appendix A for further information on sources of error and operational measures used to improve relative accuracy.

LiDAR Absolute Accuracy

Absolute accuracy was assessed using Non-Vegetated Vertical Accuracy (NVA) reporting designed to meet guidelines presented in the FGDC National Standard for Spatial Data Accuracy[3]. NVA compares known ground quality assurance point data collected on open, bare earth surfaces with level slope (<20°) to the triangulated surface generated by the LiDAR points. NVA is a measure of the accuracy of LiDAR point data in open areas where the LiDAR system has a high probability of measuring the ground surface and is evaluated at the 95% confidence interval (1.96 * RMSE), as shown in Table 11.

The mean and standard deviation (sigma σ) of divergence of the ground surface model from quality assurance point coordinates are also considered during accuracy assessment. These statistics assume the error for x, y and z is normally distributed, and therefore the skew and kurtosis of distributions are also considered when evaluating error statistics. For the California High Speed Rail – South AOI survey, 149 quality assurance points were withheld in total resulting in a non-vegetated vertical accuracy of -0.159 feet (0.049 meters) (Figure 9).

QSI also assessed absolute accuracy using 2,833 ground control points. Although these points were used in the calibration and post-processing of the LiDAR point cloud, they still provide a good indication of the overall accuracy of the LiDAR dataset, and therefore have been provided in Table 11 and Figure 10.

Table 11: Absolute accuracy results

Absolute Accuracy		
	Quality Assurance Points (NVA)	**Ground Control Points**
Sample	149 points	2,833 points
NVA (1.96*RMSE)	0.159 ft 0.049 m	0.147 ft 0.045 m
Average	-0.025 ft -0.008 m	-0.022 ft -0.007 m
Median	-0.026 ft -0.008 m	-0.023 ft -0.007 m
RMSE	0.081 ft 0.025 m	0.075 ft 0.023 m
Standard Deviation (1σ)	0.078 ft 0.024 m	0.072 ft 0.022 m

[3] Federal Geographic Data Committee, ASPRS POSITIONAL ACCURACY STANDARDS FOR DIGITAL GEOSPATIAL DATA EDITION 1, Version 1.0, NOVEMBER 2014. http://www.asprs.org/PAD-Division/ASPRS-POSITIONAL-ACCURACY-STANDARDS-FOR-DIGITAL-GEOSPATIAL-DATA.html.

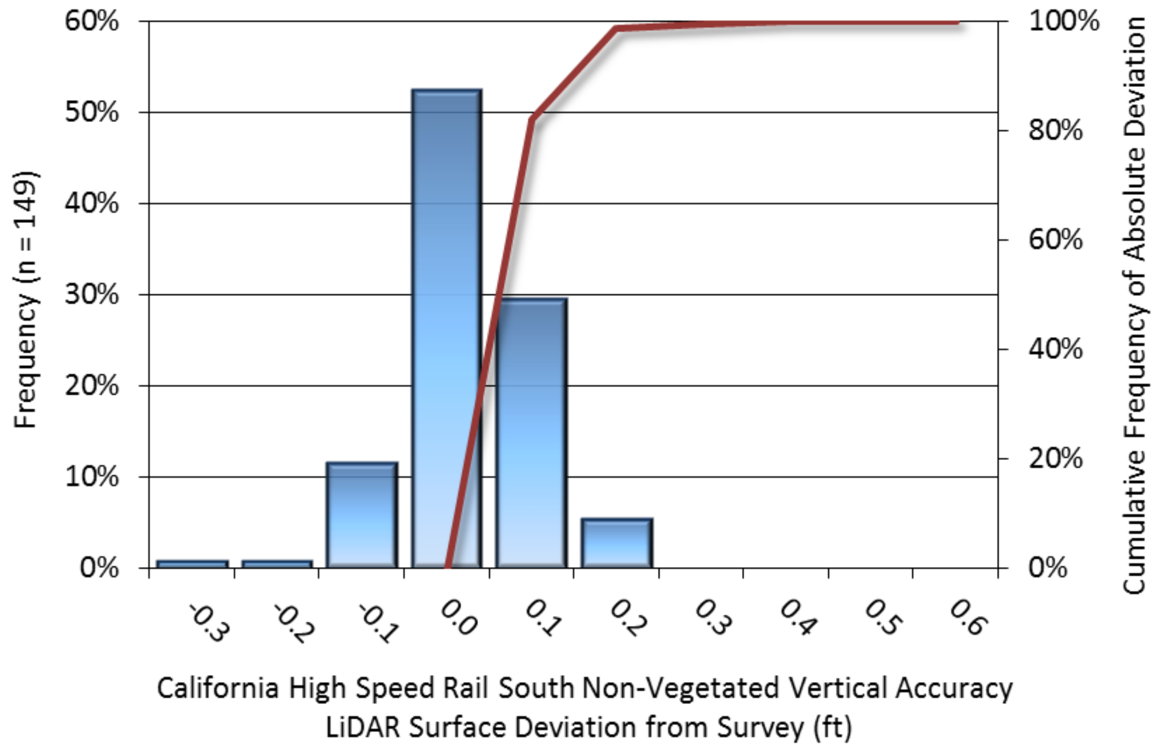

Figure 9: Frequency histogram for LiDAR surface deviation from quality assurance point values

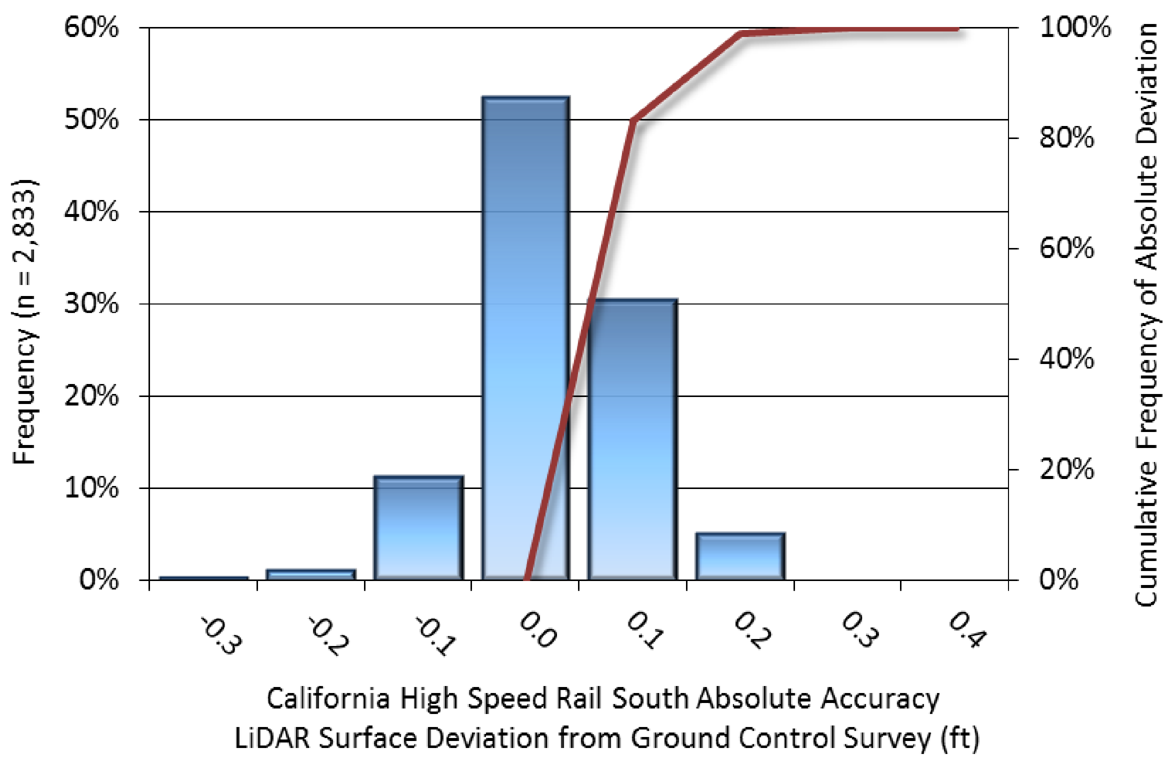

Figure 10: Frequency histogram for LiDAR surface deviation from ground control point values

LiDAR Relative Vertical Accuracy

Relative vertical accuracy refers to the internal consistency of the data set as a whole: the ability to place an object in the same location given multiple flight lines, GPS conditions, and aircraft attitudes. When the LiDAR system is well calibrated, the swath-to-swath vertical divergence is low (<0.10 meters). The relative vertical accuracy was computed by comparing the ground surface model of each individual flight line with its neighbors in overlapping regions. The average (mean) line to line relative vertical accuracy of the South AOI for the California High Speed Rail LiDAR project was 0.136 feet (0.042 meters) (Table 12, Figure 11).

Table 12: Relative accuracy results

Relative Accuracy	
Sample	424 surfaces
Average	0.136 ft 0.042 m
Median	0.135 ft 0.041 m
RMSE	0.153 ft 0.047 m
Standard Deviation (1σ)	0.051 ft 0.015 m
1.96σ	0.099 ft 0.030 m

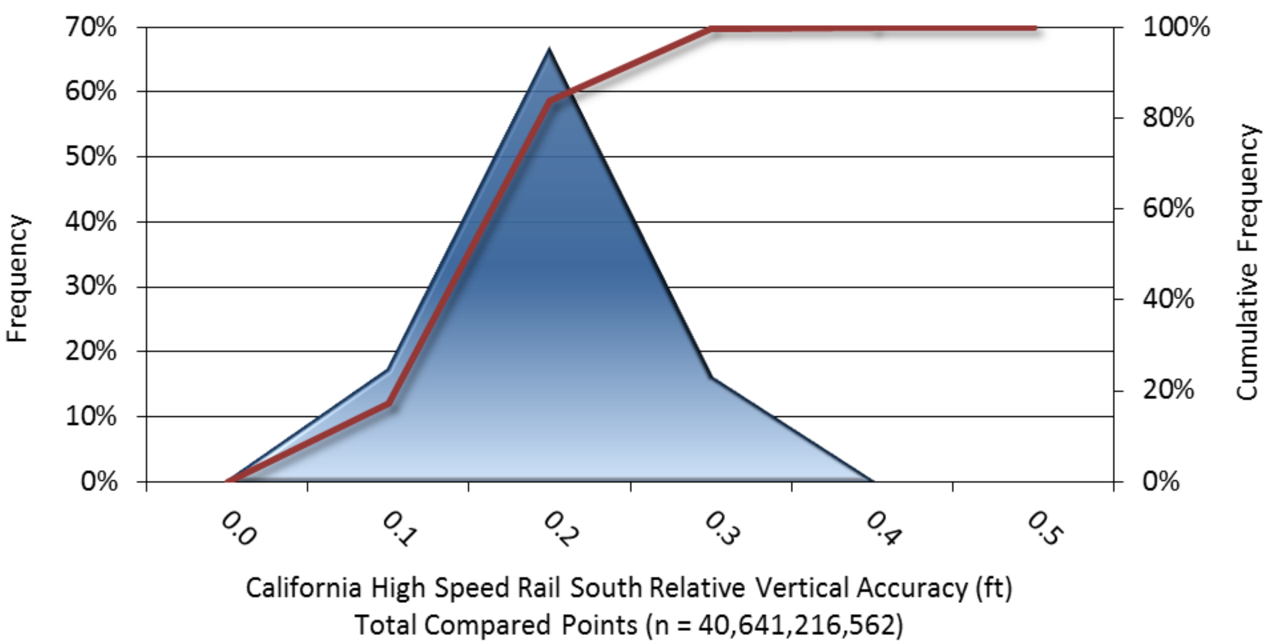

Figure 11: Frequency plot for relative vertical accuracy between flight lines

I, Thomas J. Tucker,
being duly registered as a California Land Surveyor, in the State of California, say that I certify the methodologies and results of the attached LiDAR Project (California High Speed Rail-South AOI), and that Static GNSS occupations on the Base Stations during Airborne Flights and RTK/PPK Surveys on hard surfaces were performed using commonly accepted Standard Survey Practices. Field Work commenced on August 27, 2016 and was completed on September 17, 2016.

Accuracy statistics shown in the Accuracy Section of this Report, have been reviewed by me and found to meet the "National Standard for Spatial Data Accuracy".

Thomas J. Tucker; CA PLS # 4460; Certified Photogrammetrist # R1430(ASPRS)

Remote Pilot # 3911615 (FAA); Expires: 9/06/2018.

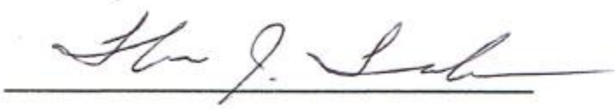

California Land Survey Manager- Quantum Spatial, Inc.

Prepared on January 13, 2017.

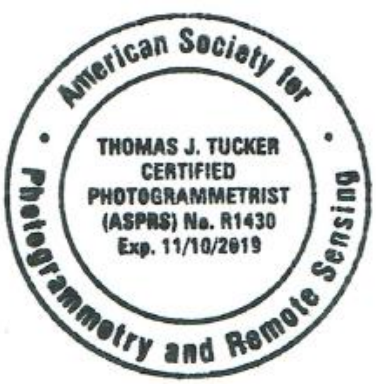

Expires on 09/30/2017

GLOSSARY

1-sigma (σ) Absolute Deviation: Value for which the data are within one standard deviation (approximately 68th percentile) of a normally distributed data set.

1.96 * RMSE Absolute Deviation: Value for which the data are within two standard deviations (approximately 95th percentile) of a normally distributed data set, based on the FGDC standards for Non-vegetated Vertical Accuracy (NVA) reporting.

Accuracy: The statistical comparison between known (surveyed) points and laser points. Typically measured as the standard deviation (sigma σ) and root mean square error (RMSE).

> **Absolute Accuracy:** The vertical accuracy of LiDAR data is described as the mean and standard deviation (sigma σ) of divergence of LiDAR point coordinates from ground survey point coordinates. To provide a sense of the model predictive power of the dataset, the root mean square error (RMSE) for vertical accuracy is also provided. These statistics assume the error distributions for x, y and z are normally distributed, and thus we also consider the skew and kurtosis of distributions when evaluating error statistics.
>
> **Relative Accuracy:** Relative accuracy refers to the internal consistency of the data set; i.e., the ability to place a laser point in the same location over multiple flight lines, GPS conditions and aircraft attitudes. Affected by system attitude offsets, scale and GPS/IMU drift, internal consistency is measured as the divergence between points from different flight lines within an overlapping area. Divergence is most apparent when flight lines are opposing. When the LiDAR system is well calibrated, the line-to-line divergence is low (<10 cm).
>
> **Root Mean Square Error (RMSE):** A statistic used to approximate the difference between real-world points and the LiDAR points. It is calculated by squaring all the values, then taking the average of the squares and taking the square root of the average.

Data Density: A common measure of LiDAR resolution, measured as points per square meter.

Digital Elevation Model (DEM): File or database made from surveyed points, containing elevation points over a contiguous area. Digital terrain models (DTM) and digital surface models (DSM) are types of DEMs. DTMs consist solely of the bare earth surface (ground points), while DSMs include information about all surfaces, including vegetation and man-made structures.

Intensity Values: The peak power ratio of the laser return to the emitted laser, calculated as a function of surface reflectivity.

Nadir: A single point or locus of points on the surface of the earth directly below a sensor as it progresses along its flight line.

Overlap: The area shared between flight lines, typically measured in percent. 100% overlap is essential to ensure complete coverage and reduce laser shadows.

Pulse Rate (PR): The rate at which laser pulses are emitted from the sensor; typically measured in thousands of pulses per second (kHz).

Pulse Returns: For every laser pulse emitted, the number of wave forms (i.e., echos) reflected back to the sensor. Portions of the wave form that return first are the highest element in multi-tiered surfaces such as vegetation. Portions of the wave form that return last are the lowest element in multi-tiered surfaces.

Real-Time Kinematic (RTK) Survey: A type of surveying conducted with a GPS base station deployed over a known monument with a radio connection to a GPS rover. Both the base station and rover receive differential GPS data and the baseline correction is solved between the two. This type of ground survey is accurate to 1.5 cm or less.

Post-Processed Kinematic (PPK) Survey: GPS surveying is conducted with a GPS rover collecting concurrently with a GPS base station set up over a known monument. Differential corrections and precisions for the GNSS baselines are computed and applied after the fact during processing. This type of ground survey is accurate to 1.5 cm or less.

Scan Angle: The angle from nadir to the edge of the scan, measured in degrees. Laser point accuracy typically decreases as scan angles increase.

Native LiDAR Density: The number of pulses emitted by the LiDAR system, commonly expressed as pulses per square meter.

Relative Accuracy Calibration Methodology:

Manual System Calibration: Calibration procedures for each mission require solving geometric relationships that relate measured swath-to-swath deviations to misalignments of system attitude parameters. Corrected scale, pitch, roll and heading offsets were calculated and applied to resolve misalignments. The raw divergence between lines was computed after the manual calibration was completed and reported for each survey area.

Automated Attitude Calibration: All data were tested and calibrated using TerraMatch automated sampling routines. Ground points were classified for each individual flight line and used for line-to-line testing. System misalignment offsets (pitch, roll and heading) and scale were solved for each individual mission and applied to respective mission datasets. The data from each mission were then blended when imported together to form the entire area of interest.

Automated Z Calibration: Ground points per line were used to calculate the vertical divergence between lines caused by vertical GPS drift. Automated Z calibration was the final step employed for relative accuracy calibration.

LiDAR accuracy error sources and solutions:

Type of Error	Source	Post Processing Solution
GPS (Static/Kinematic)	Long Base Lines	None
	Poor Satellite Constellation	None
	Poor Antenna Visibility	Reduce Visibility Mask
Relative Accuracy	Poor System Calibration	Recalibrate IMU and sensor offsets/settings
	Inaccurate System	None
Laser Noise	Poor Laser Timing	None
	Poor Laser Reception	None
	Poor Laser Power	None
	Irregular Laser Shape	None

Operational measures taken to improve relative accuracy:

Low Flight Altitude: Terrain following was employed to maintain a constant above ground level (AGL). Laser horizontal errors are a function of flight altitude above ground (about 1/3000th AGL flight altitude).

Focus Laser Power at narrow beam footprint: A laser return must be received by the system above a power threshold to accurately record a measurement. The strength of the laser return (i.e., intensity) is a function of laser emission power, laser footprint, flight altitude and the reflectivity of the target. While surface reflectivity cannot be controlled, laser power can be increased and low flight altitudes can be maintained.

Reduced Scan Angle: Edge-of-scan data can become inaccurate. The scan angle was reduced to a maximum of $\pm 20^{o}$ from nadir, creating a narrow swath width and greatly reducing laser shadows from trees and buildings.

Quality GPS: Flights took place during optimal GPS conditions (e.g., 6 or more satellites and PDOP [Position Dilution of Precision] less than 3.0). Before each flight, the PDOP was determined for the survey day. During all flight times, a dual frequency DGPS base station recording at 1 second epochs was utilized and a maximum baseline length between the aircraft and the control points was less than 13 nm at all times.

Ground Survey: Ground survey point accuracy (<1.5 cm RMSE) occurs during optimal PDOP ranges and targets a minimal baseline distance of 4 miles between GPS rover and base. Robust statistics are, in part, a function of sample size (n) and distribution. Ground survey points are distributed to the extent possible throughout multiple flight lines and across the survey area.

50% Side-Lap (100% Overlap): Overlapping areas are optimized for relative accuracy testing. Laser shadowing is minimized to help increase target acquisition from multiple scan angles. Ideally, with a 50% side-lap, the nadir portion of one flight line coincides with the swath edge portion of overlapping flight lines. A minimum of 50% side-lap with terrain-followed acquisition prevents data gaps.

Opposing Flight Lines: All overlapping flight lines have opposing directions. Pitch, roll and heading errors are amplified by a factor of two relative to the adjacent flight line(s), making misalignments easier to detect and resolve.